Development Design of a Compact Pulsed Electric Field to Reduce Food Bacteria: Laboratory Scale

Arry Darmawan
Department of Food Science and Technology, IPB University, Bogor, Indonesia
profarry@apps.ipb.ac.id

Nur Wulandari
Department of Food Science and Technology, IPB University, Bogor, Indonesia
wulandari_n@apps.ipb.ac.id (corresponding author)

Harsi Dewantari Kusumaningrum
Department of Food Science and Technology, IPB University, Bogor, Indonesia
h_kusumaningrum@apps.ipb.ac.id

Siti Nurjanah
Department of Food Science and Technology, IPB University, Bogor, Indonesia
sity_nr@apps.ipb.ac.id

Anto Tri Sugiarto
Research Center for OREI Technology, National Research and Innovation Agency, Bandung, Indonesia
anto008@brin.go.id

Qirom Qirom
Electronics Engineering Department, Politeknik Harapan Bersama, Tegal, Indonesia
qirom.bahagia2@gmail.com

Adji Parikesit
Research Center for OREM, National Research and Innovation Agency, Tangerang, Indonesia
adji003@brin.go.id

Astu Unadi
Research Center for OREM, National Research and Innovation Agency, Tangerang, Indonesia
astu004@brin.go.id

Sabirin Sabirin
Research Center for Agroindustry, National Research and Innovation Agency, Tangerang, Indonesia
sabi001@brin.go.id

Received: 26 May 2025 | Revised: 30 June 2025, 12 July 2025, 17 July 2025, 21 July 2025, and 31 July 2025 | Accepted: 2 August 2025

 DOI: https://doi.org/10.48084/etasr.12377

ABSTRACT

This study aims to design a high-efficiency Pulsed Electric Field (PEF) device for bacterial inactivation in food at a laboratory scale. Bacterial inactivation is closely affected by the consistency, intensity, and duration of the applied electric field; thus, although multiple circuit topologies can be employed in PEF

devices, not all provide compactness and efficiency. For this study, an iterative design approach was used to evaluate solid-state cascade PEF topologies by comparing transformer-based (2 A and 5 A) and ignition coil-based (mini-cylinder, cylinder, and canister) configurations. The results show that PEF devices employing a 2 A transformer current and a mini-cylindrical ignition coil offer superior reliability and compactness, making them suitable for treating liquid, semi-solid, and solid samples. Experimental validation of the PEF effect on bacterial membrane damage, using the *Vibrio parahaemolyticus* strain, demonstrated that an electric field intensity of 10.5 kV/cm caused significant cell damage. Extended treatment durations led to progressively higher bacterial mortality ($p < 0.05$), as confirmed by flow cytometry and Scanning Electron Microscope (SEM) observations of cell morphology. Therefore, this study successfully developed a PEF device that potentially replaces the traditional Pulse Forming Network (PFN) with a mini-cylindrical ignition coil, thereby improving replicability and accessibility for laboratory-scale applications.

Keywords-Pulsed Electric Field (PEF); laboratory scale; solid-state cascade; bacterial inactivation; food

I. INTRODUCTION

Pulsed Electric Field (PEF) technology has attracted scientific interest as a non-thermal method for inactivating harmful bacteria in food by applying short-duration pulses (μs to ms) of 10-25 kV/cm intensity and 5-10 A current, which damages cell membranes [1]. PEF applications have been widely investigated for various types of liquid, semi-liquid, and solid foods [2], with effectiveness depending on process parameters (electric field strength, duration, specific energy, pulse shape, width, frequency, and temperature), sample characteristics (pH, and conductivity), and microbial properties (cell size, cell morphology, and membrane structure) [3].

The selection of electrical topology plays a significant role in PEF device development, particularly for laboratory research. In this study, the cascaded solid-state topology was selected due to its compact design [4], operational efficiency, and improved safety, achieved by gradually increasing output voltage through multiple semiconductor stages, thereby reducing voltage stress per switch [5]. This approach offers advantages over other topologies, including transmission line pulsers [6], transformer-based systems [7], gaseous switch circuits [8], solid-state H-bridges [9], and Marx banks [10]. Nevertheless, the lack of detailed documentation and component availability in PEF manufacturing makes replicating the device in laboratory settings particularly challenging [11].

To address this, the present study, investigating a cascaded solid-state topology, follows an iterative design process. The system employs an ignition coil as a high-voltage booster and is suitable for liquid, semi-solid, and solid samples. Inactivation tests were performed on *Vibrio parahaemolyticus*, a marine pathogen known for heat resistance, biofilm formation, and salinity tolerance [12], commonly associated with raw or undercooked seafood [13]. The developed PEF device can potentially replace the traditional Pulse Forming Network (PFN) with an ignition coil and a Current Transformer (CT), enhancing replicability. Its compact architecture and reliance on commercially available components make it practical for laboratory applications.

II. MATERIALS AND METHODS

A. Materials

1) PEF Device

The PEF device used in this study was designed with a solid-state cascaded topology employing Metal Oxide Semiconductor Field Effect Transistors (MOSFETs). Its main components included an Alternating Current (AC) power input, a step-down CT, a diode bridge for AC-Direct Current (DC) conversion, a DC LM2596 buck converter module, an NE555 integrated circuit (pulse generator), an ignition coil for voltage step-up, a voltage regulator module for voltage stabilization, and an optocoupler for signal control and isolation.

2) Testing Equipment

The experimental setup incorporated an oscilloscope (Tektronix TBS 1062), a thermometer gun, an acoustic camera (Fluke ii910), a flow cytometer (BD Attune Plus, Biosciences, USA), and a Scanning Electron Microscope (SEM) (Thermo Scientific Prisma E, USA).

3) Chemicals and Biological Materials

The chemicals and biological materials used were Aquadest, *Vibrio parahaemolyticus* ATCC 17802 (Thermo Fisher Scientific, USA), Phosphate-Buffered Saline (PBS) (Oxoid, UK), Tryptic Soy Broth (TSB) (Oxoid, UK), and Propidium Iodide (PI) (Sysmex, Japan).

B. Methods

The study comprised four main stages in assembling the PEF system:

- Selection of a cascaded solid-state topology as the system foundation.
- Design of the electrical circuit.
- Iterative selection and assembly of components, beginning with performance comparisons of transformers and ignition coils, followed by long-duration durability testing of the selected components.
- Testing of electrical output characteristics and evaluation of the PEF system's effectiveness in inactivating V. parahaemolyticus.

1) Assembly of Voltage and Pulse Generator

At this stage, transformers (2 A and 5 A) and ignition coils (mini-cylinder, cylinder, and canister) were tested. Component stability was assessed based on temperature increase (<75 ℃) [14]. Reliability was evaluated through a 240-minute life test on transistors, ignition coils, and MOSFETs [15]. Furthermore,

integration into the treatment chamber was tested by connecting the generator to the treatment chamber, monitoring electrical output with the Fluke ii910 acoustic camera, determining optimal electrode spacing based on breakdown voltage, and recording temperature rise with a thermometer gun for 60 minutes at maximum voltage.

2) Testing PEF Output and Antibacterial Effectiveness

PEF performance and antibacterial activity were evaluated by assessing bacterial membrane damage and morphology [16]. The target strain, *V. parahaemolyticus* ATCC 17802, was cultured in TSB medium. Experimental groups included untreated controls and PEF-treated samples (10, 20, and 30 s). Cultures were centrifuged at 9000 rpm for 15 min at 4 ℃ with sterile PBS. Samples were stained with 0.5 µL PI per 0.5 mL suspension and analyzed by flow cytometry (maximum wavelength 605 nm). The percentage of bacterial cell damage was calculated to determine optimal treatment [17], targeting 99% cell death, using (1):

$$N_{(t)} = N_0 \cdot (1 + r)^{t/T} \quad (1)$$

where:

- $N_{(t)}$: value at time t (s),
- N_0: initial cell count (at $t = 10$ s, since data collection began at 10 s),
- r: rate of change per interval (2.3% per 10 s),
- T: fixed time interval (10 s),
- t: time in s.

3) SEM Observation of Bacterial Morphology

SEM analysis followed a modified procedure in [18]. Bacterial suspensions were washed with 0.1 M PBS, fixed with 2.5% glutaraldehyde and 4% paraformaldehyde, post-fixed with 1% osmium tetroxide, dehydrated, and immersed in epoxy resin [19]. Observations were conducted at 10,000× magnification, 10.9 mm working distance, and 10 kV voltage.

4) Statistical Analysis

Statistical analyses were conducted using a Completely Randomized Design (CRD) without grouping. Factors included:

- PEF reliability analysis: duration of use of different ignition coil components.
- Treatment chamber heating: duration of exposure at constant voltage.
- Bacterial reduction: four treatments (control, 10.5 kV/cm for 10, 20, and 30 s).

Overall, each statistical analysis used a one-way Analysis of Variance (ANOVA) method at a 95% confidence interval ($\alpha = 0.05$).

III. RESULTS AND DISCUSSION

Pulse power generators have been applied in diverse fields, including PEF technology, but their design remains challenging due to the need for operational consistency and cost efficiency at an industrial scale [20]. Several studies have proposed efficient high-power pulse generators for PEF applications [21], emphasizing energy efficiency, operator safety, and affordability [22].

In this study, the generator design employed an H-bridge and MOSFET-based cascaded solid-state pulse generator topology. This topology gradually increases the output voltage through multiple semiconductors switching stages, thereby improving reliability, reducing voltage stress on individual switches, and enhancing overall system safety [10]. Solid-state cascaded topologies are particularly suitable for PEF applications [11] because stacked medium-power switches can withstand high power without requiring a single high-power switch, ultimately reducing design cost [7]. The PCB design resulting from the solid-state cascaded topology is shown in Figure 1.

The working principle begins with the power input through components 1 and 2, which use separate power supplies to isolate the NE555 IC from the ignition coil. The current is rectified by a diode (component 3) to convert AC into DC and then stabilized at 5 V using a 7805-voltage regulator. The NE555 timer IC (component 4) generates adjustable pulse frequencies controlled by a potentiometer (component 5), while a Light Emitting Diode (LED) indicator (component 6) displays operational status. The signal is isolated by an optocoupler (component 7) to minimize electrical interference, amplified through a MOSFET (component 8), and delivered to the ignition coil (component 9), which produces the required high-voltage pulses for the PEF process.

Transformer selection (step-down and step-up) was based on high efficiency (up to 95%) and commercial availability [23]. The ignition coil was selected for its compact design, rapid voltage rise via electromagnetic induction, and affordability, making it preferable to alternatives such as flyback transformers, Marx generators, or PFNs [10]. The experimental setup is shown in Figure 2.

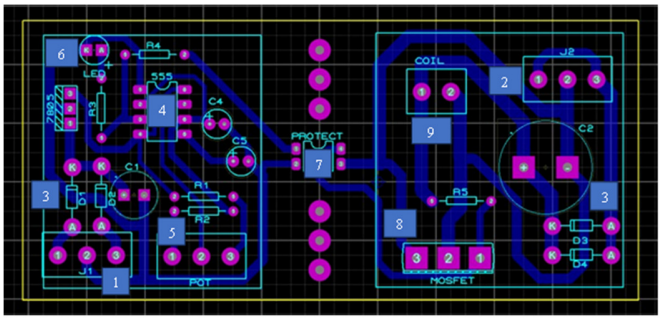

Fig. 1. Solid-state cascaded PCB design: Dimension 5x6 cm; (1) and (2) mains input; (3) rectifier diode; (4) NE555 IC; (5) potentiometer; (6) indicator LED; (7) optocoupler jumper; (8) MOSFET; (9) ignition coil.

A. Performance of Ignition Coils and Transformer

The transformer evaluated the circuit board's power supply performance and output stability under different current strengths, while the ignition coil functioned to step up the input

voltage from 12 V to as high as 25 kV or more, depending on ambient pressure and charging time [24]. Figure 3 shows that a 2 A transformer provided the best runtime performance. Moreover, both the mini-cylindrical and cylindrical ignition coils operated for 6 ± 0.01 hours without significant differences ($p > 0.05$), whereas the canister coil lasted only 2 ± 0.02 hours, a significant reduction ($p < 0.05$). In contrast, when a 5 A transformer was used, all three coil types exhibited reduced runtimes of 3 ± 0.01 hours, with no significant differences among them ($p > 0.05$).

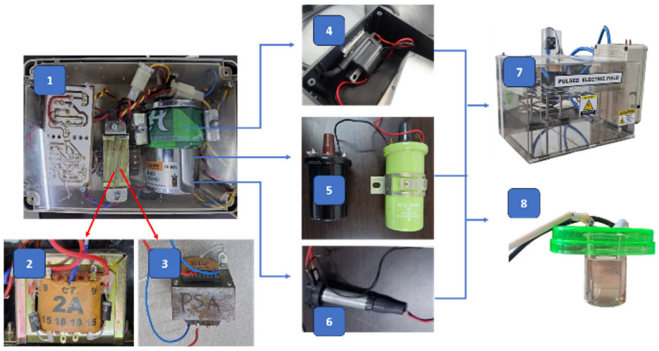

Fig. 2. Experimental PEF circuit with various components: (1) high voltage PEF generator circuit; (2) transformer 2 A; (3) transformer 5 A; (4) mini cylinder ignition coil; (5) canister ignition coil; (6) cylinder ignition coil; (7) electrode plate in the treatment chamber; (8) tube electrode.

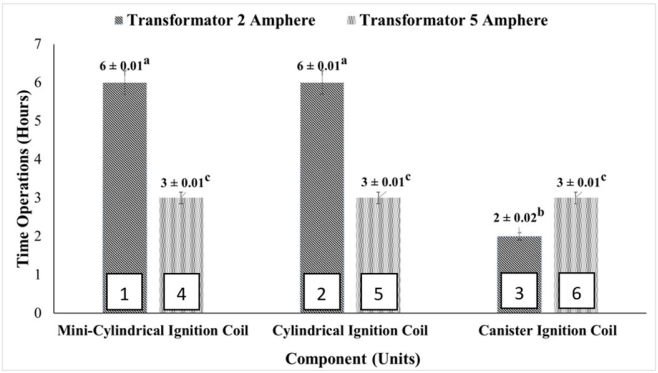

Fig. 3. Comparison of operating time (h) of three types of ignition coils (mini-cylindrical, cylindrical, and canister) on two types of transformers (2 A and 5 A current). Different superscript letters (a-c) indicate statistically significant differences.

Damage analysis of units 3-6 revealed different failure mechanisms. In unit 3, the 2 A transformer provided insufficient current, resulting in longer charging times, lower secondary induction voltage, and excessive transistor switching stress. This combination limited high-voltage generation [25] and caused thermal stress on the canister-type ignition coil [26]. In unit 4, the mini-cylindrical coil failed due to excessive current from the 5 A transformer, leading to overheating, winding insulation breakdown, and eventually to short-circuiting [27]. In unit 5, overvoltage and current surges caused transistor breakdown and MOSFET burnout [28]. Finally, unit 6 suffered damage because the 5 A transformer exceeded the regulator's safe input voltage, resulting in overheating, diode and MOSFET failure due to thermal stress and reverse current [29], and ignition coil inefficiency caused by magnetic saturation [30] and copper winding degradation [28]. To address these issues, iterative modifications were implemented, including widening the PCB dimensions to 5×10 cm and upgrading high-voltage optocouplers to better protect against heat surges and overvoltage. Following these adjustments, in-depth tests were conducted focusing on MOSFETs, ignition coils, and transistors. Unit 1 demonstrated stable operation for 240 minutes across three replicates, with no significant temperature increase. Table I summarizes the experimental outcomes.

While unit 2 achieved high voltage output, its reliability was limited to ~200 minutes, with MOSFET temperatures exceeding 75 °C, indicating thermal failure. MOSFETs are particularly vulnerable to overheating, high-voltage stress, and electromagnetic interference, all common in PEF systems [31]. Among all tested designs, unit 1 (2 A transformer + mini-cylindrical coil) demonstrated the best balance of reliability, compactness, and efficiency. Its favorable primary-secondary winding ratio and ferromagnetic core contributed to efficient voltage gain, accelerated induction, and reduced magnetic reluctance [24].

TABLE I. PEF CIRCUIT EXPERIMENT OF DIFFERENT TYPES OF COMPONENTS

Unit	Transformer	Ignition coil	Voltage output and endurance time
1	2 A	Mini-cylindrical	6 h stable at 25.8 kV
2	2 A	Cylindrical	6 h stable at 50 kV
3	2 A	Canister	2 h at 50 kV, then coil was damaged
4	5 A	Mini-cylindrical	3 h at 25.8 kV, then coil burned
5	5 A	Cylindrical	3 h at 50 kV, then MOSFET burned
6	5 A	Canister	3 h at 50 kV, then transformer, diode, MOSFET, and coil were damaged

These results suggest that the mini-cylindrical ignition coil offers the most practical option for laboratory-scale PEF applications. Its compact form factor, stable endurance, and efficient performance make it suitable for treating liquid, semi-solid, and solid food samples. For industrial applications, parameters such as PCB dimensions, grounding strategies, ignition coil selection, and treatment chamber conductivity settings can be adjusted to optimize the applied electric field.

B. PEF Output Characteristics

The waveform generated by unit 1 was suitable for PEF applications, as confirmed by square pulses with rapid rising and falling edges at the mini-cylindrical ignition coil (input) and the anode (output). Square pulses were selected because they maximize treatment efficiency while minimizing temperature rise [20]. The measured PEF specifications included an anode voltage of 25.8 kV, frequency of 683-702 Hz (stable at 684 Hz), pulse duration of 400 µs, and current of 2 A. Test results are presented in Figure 4.

Thermal stability was evaluated using a thermo-gun under vacuum for 30 minutes. During a continuous 60-minute

treatment, the PEF chamber temperature did not increase by more than 30 ℃, confirming compliance with the standard for non-thermal PEF technology. Electrode spacing is a critical factor in determining electric field strength, expressed as:

$$E = \frac{V}{d} \quad (2)$$

where E is the electric field strength, V the applied voltage, and d the electrode distance [10]. Excessive spacing reduces ionization efficiency, as the voltage may be insufficient to ionize the air, thereby weakening the electric field [32]. Optimal performance is achieved when electrode spacing enables the electric field to exceed the breakdown voltage of air (~3 kV/mm under standard conditions), producing ionization and establishing a conductive discharge path [23].

Experimental results demonstrated that at an electrode distance of 2.45 cm, the system generated a strong electric field of approximately ±10.5 kV/cm, sufficient to ionize air and produce a stable discharge. Thus, excessive electrode spacing inhibits effective PEF treatment, except in high-conductivity media [23]. Electrode spacing determination is illustrated in Figure 5.

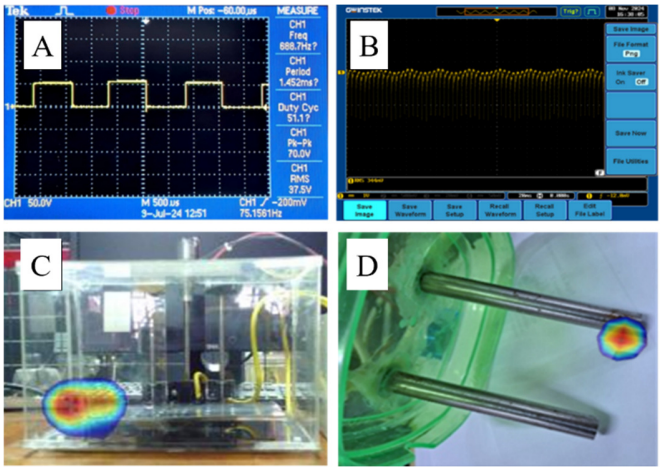

Fig. 4. Waveforms and corona discharges of PEF electrodes. (A) input pulsed waveform; (B) pulsed waveform of PEF output; (C) corona discharge electrode plate; (D) corona discharge electrode cylindrical bar.

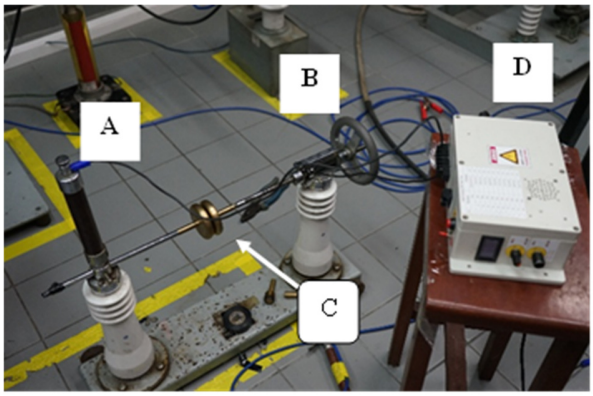

Fig. 5. Testing electrode spacing based on electrical breakdown testing the optimum distance between electrodes with (A) anode; (B) cathode; (C); electrode spacing performed; (D) PEF high voltages.

C. Effect of PEF on Bacterial Cell Damage

The mechanism of bacterial cell reduction of *V. parahaemolyticus* was evaluated by examining cell membrane damage under an electric field of 10.5 kV/cm applied for 10, 20, and 30 s. Flow cytometry analysis was performed using dot density plots (Figure 6) based on the Forward Scatter Area (FSC-A) and Side Scatter Area (SSC-A) parameters, representing cell size and internal complexity (granularity). The percentage of damaged or dead cells is summarized in Table II.

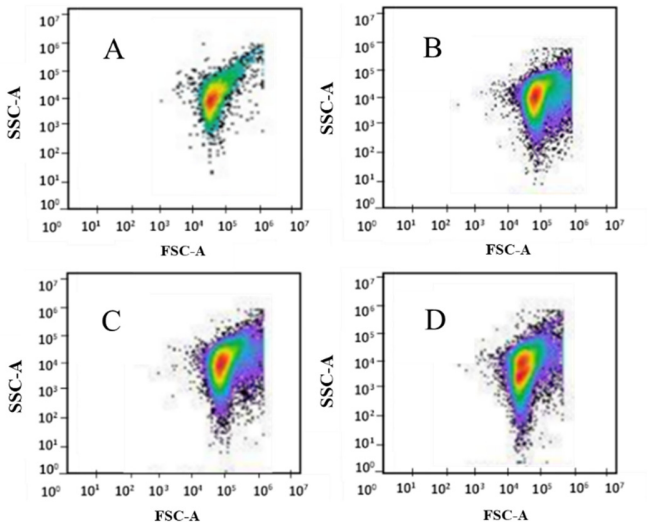

Fig. 6. Observation results of bacterial cell scatter detected by flow cytometer. FSC-A and SSC-A (log scale), (A) control sample; (B) PEF 10.5 kV/cm (10 s); (C) PEF 10.5 kV/cm (20 s); (D) PEF 10.5 kV (30 s). Red color indicates bacterial cell death (R1).

TABLE II. RESULTS OF PEF TREATMENT OF BACTERIAL CELLS ON A FLOW CYTOMETER

Sample and treatment	Total cells (Log cell/ 0.5 mL)		Average damaged cells (%)
	Number of cells Detected	Number of Damaged cells	
Control	4.33 ± 0.6	2.41 ± 0.002	2.6 ± 0.01[a]
Sample 10.5 kV/cm (10 s)	5.08 ± 0.01	4.55 ± 0.01	29.39 ± 0.13[b]
Sample 10.5 kV/cm (20 s)	5.08 ± 0.01	4.58 ± 0.01	31.66 ± 0.14[c]
Sample 10.5 kV/cm (30 s)	5.08 ± 0.01	4.61 ± 0.01	34.11 ± 0.2[d]

Different superscript letters (a-d) indicate significant differences ($p<0.05$).

The flow cytometer results of the untreated control (A) showed 2.6% of cells within the R1 gate exhibiting high membrane permeability, indicating natural stress-related damage [33]. In comparison, 29.39%, 31.66%, and 34.11% of cells were damaged in samples (B), (C), and (D), corresponding to treatments of 10, 20, and 30 s, respectively. The results confirm that prolonged PEF exposure significantly increased bacterial cell death ($p<0.05$).

Irreversible bacterial membrane damage typically requires electric fields >10 kV/cm. Gram-negative bacteria such as *V. parahaemolyticus* are effectively inactivated in the 8-12 kV/cm

range, whereas Gram-positive bacteria generally require stronger fields (>15 kV/cm) [35]. The required field strength also depends on sample conductivity, which is influenced by food matrix components such as ions, salts, and proteins [34]. Based on Table II data and mathematical modeling, achieving a 99% reduction would require approximately 245 s (4 min and 5 s) of PEF treatment under the same conditions.

D. Bacterial Cell Damage Observed Using SEM

SEM analysis confirmed membrane disruption in *V. parahaemolyticus* cells subjected to PEF treatment. The control sample (Figure 7(A)) showed intact rod-shaped cells without visible damage. After treatment at 10.5 kV/cm for 10 and 20 s (Figures 7(B) and 7(C)), pore formation was evident in the membranes, though some cells exhibited sublethal injury consistent with previous studies [35]. At 30 s (Figure 7(D)), electroporation effects were more pronounced, leading to irreversible membrane damage, increased permeability, and collapse of normal cell morphology, as similarly reported in earlier research [35].

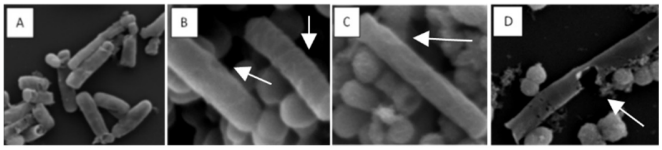

Fig. 7. Cell morphology of *V. parahaemolyticus* at various PEF treatments. (A) intact cell; (B) 10.5 kV/cm 10 s PEF treated cell; (C) 10.5 kV/cm 20 s PEF treated cell; (D) 10.5 kV/cm 30 s PEF treated cell.

These findings demonstrate that the cascaded solid-state PEF system with transformer-based step-up/step-down regulation and a mini-cylindrical ignition coil provides reliable high-voltage generation. The optimized unit 1 design (2 A transformer, voltage regulator, NE555 IC, optocoupler, diode, MOSFET, and ignition coil) proved effective for compact laboratory-scale PEF applications. Furthermore, the use of cylindrical bar electrodes with output monitoring via the Fluke ii90 acoustic camera confirmed uniform conductivity within the treatment chamber, supporting batch-mode application for liquid, semi-solid, and solid food samples.

IV. CONCLUSION

This study successfully developed a laboratory-scale Pulsed Electric Field (PEF) system based on a cascaded solid-state topology, demonstrating a compact, reliable, and versatile design suitable for liquid, semi-solid, and solid food samples. Reliability testing indicated that combining a 2 A transformer with a mini-cylinder ignition coil provided stable high-voltage output, while the generated waveform consisted of efficient square pulses. Experimental results showed that PEF treatment at an electric field of 10.5 kV/cm, with a tube electrode spacing of 2.45 cm, effectively damaged the cell membrane of Vibrio parahaemolyticus. These findings highlight that cascaded solid-state PEF devices offer a practical, cost-effective, and reproducible approach for laboratory-scale food research and microbial inactivation applications.

REFERENCES

[1] U. U. Nabilah, A. B. Sitanggang, R. Dewanti-Hariyadi, A. T. Sugiarto, and E. H. Purnomo, "Meta-analysis: microbial inactivation in milk using pulsed electric field," *International Journal of Food Science & Technology*, vol. 57, no. 9, pp. 5750–5763, Sep. 2022, https://doi.org/10.1111/ijfs.15942.

[2] Z. F. Bhat, J. D. Morton, S. L. Mason, and A. E.-D. A. Bekhit, "Pulsed electric field operates enzymatically by causing early activation of calpains in beef during ageing," *Meat Science*, vol. 153, pp. 144–151, Jul. 2019, https://doi.org/10.1016/j.meatsci.2019.03.018.

[3] S. Mahnič-Kalamiza and D. Miklavčič, "The Phenomenon of Electroporation," in *Pulsed Electric Fields Technology for the Food Industry*, J. Raso, V. Heinz, I. Alvarez, and S. Toepfl, Eds. Cham: Springer International Publishing, 2022, pp. 107–141.

[4] J. Rao, Y. Lei, S. Jiang, Z. Li, and J. F. Kolb, "All Solid-State Rectangular Sub-Microsecond Pulse Generator for Water Treatment Application," *IEEE Transactions on Plasma Science*, vol. 46, no. 10, pp. 3359–3363, Oct. 2018, https://doi.org/10.1109/TPS.2018.2829206.

[5] S. Li, J. Gao, M. Sack, H. Yang, B. Qian, and G. Mueller, "Study on a Solid-State Pulse Generator Based on Magnetic Switch for Food Treatments by Pulsed Electric Field (PEF)," in *1st World Congress on Electroporation and Pulsed Electric Fields in Biology, Medicine and Food & Environmental Technologies*, Singapore, 2016, vol. 53, pp. 55–59, https://doi.org/10.1007/978-981-287-817-5_13.

[6] A. A. Elserougi, A. M. Massoud, and S. Ahmed, "A Unipolar/Bipolar High-Voltage Pulse Generator Based on Positive and Negative Buck–Boost DC–DC Converters Operating in Discontinuous Conduction Mode," *IEEE Transactions on Industrial Electronics*, vol. 64, no. 7, pp. 5368–5379, Jul. 2017, https://doi.org/10.1109/TIE.2017.2677361.

[7] M. A. Elgenedy, A. Darwish, S. Ahmed, and B. W. Williams, "A Transition Arm Modular Multilevel Universal Pulse-Waveform Generator for Electroporation Applications," *IEEE Transactions on Power Electronics*, vol. 32, no. 12, pp. 8979–8991, Dec. 2017, https://doi.org/10.1109/TPEL.2017.2653243.

[8] X. Chen, L. Yu, T. Jiang, H. Tian, K. Huang, and J. Wang, "A High-Voltage Solid-State Switch Based on Series Connection of IGBTs for PEF Applications," *IEEE Transactions on Plasma Science*, vol. 45, no. 8, pp. 2328–2334, Aug. 2017, https://doi.org/10.1109/TPS.2017.2713781.

[9] M. S. Moonesan and S. H. Jayaram, "Effect of Pulsewidth on Medium Temperature Rise and Microbial Inactivation Under Pulsed Electric Field Food Treatment," *IEEE Transactions on Industry Applications*, vol. 49, no. 4, pp. 1767–1772, Jul. 2013, https://doi.org/10.1109/TIA.2013.2256411.

[10] J. Raso, V. Heinz, I. Alvarez, and S. Toepfl, Eds., *Pulsed Electric Fields Technology for the Food Industry: Fundamentals and Applications*. Cham: Springer International Publishing, 2022.

[11] R. N. Arshad *et al.*, "Electrical systems for pulsed electric field applications in the food industry: An engineering perspective," *Trends in Food Science & Technology*, vol. 104, pp. 1–13, Oct. 2020, https://doi.org/10.1016/j.tifs.2020.07.008.

[12] S. Chimalapati, A. E. Lafrance, L. Chen, and K. Orth, "*Vibrio parahaemolyticus* : Basic Techniques for Growth, Genetic Manipulation, and Analysis of Virulence Factors," *Current Protocols in Microbiology*, vol. 59, no. 1, Dec. 2020, Art. no. e131, https://doi.org/10.1002/cpmc.131.

[13] S. Hackbusch, A. Wichels, L. Gimenez, H. Döpke, and G. Gerdts, "Potentially human pathogenic Vibrio spp. in a coastal transect: Occurrence and multiple virulence factors," *Science of The Total Environment*, vol. 707, Mar. 2020, Art. no. 136113, https://doi.org/10.1016/j.scitotenv.2019.136113.

[14] A. S. Sedra and K. C. Smith, *Microelectronic circuits*, 5th ed. New York: Oxford University Press, 2010.

[15] F. Pascual, "Accelerated Life Test Planning With Independent Weibull Competing Risks," *IEEE Transactions on Reliability*, vol. 57, no. 3, pp. 435–444, Sep. 2008, https://doi.org/10.1109/TR.2008.928205.

[16] T. Falcioni, S. Papa, R. Campana, A. Manti, M. Battistelli, and W. Baffone, "State transitions of *Vibrio parahaemolyticus* VBNC cells

evaluated by flow cytometry," *Cytometry Part B: Clinical Cytometry*, vol. 74B, no. 5, pp. 272–281, Sep. 2008, https://doi.org/10.1002/cyto.b.20427.

[17] M. Feurhuber, R. Neuschwander, T. Taupitz, C. Frank, C. Hochenauer, and V. Schwarz, "Mathematically modelling the inactivation kinetics of Geobacillus stearothermophilus spores: Effects of sterilization environments and temperature profiles," *Physics in Medicine*, vol. 13, Jun. 2022, Art. no. 100046, https://doi.org/10.1016/j.phmed.2021.100046.

[18] S.-Y. Chen, W.-N. Jane, Y.-S. Chen, and H. Wong, "Morphological changes of Vibrio parahaemolyticus under cold and starvation stresses," *International Journal of Food Microbiology*, vol. 129, no. 2, pp. 157–165, Feb. 2009, https://doi.org/10.1016/j.ijfoodmicro.2008.11.009.

[19] A. R. Spurr, "A low-viscosity epoxy resin embedding medium for electron microscopy," *Journal of Ultrastructure Research*, vol. 26, no. 1–2, pp. 31–43, Jan. 1969, https://doi.org/10.1016/S0022-5320(69)90033-1.

[20] M. A. Kempkes, "Industrial Pulsed Electric Field Systems," in *Handbook of Electroporation*, D. Miklavcic, Ed. Cham: Springer International Publishing, 2017, pp. 1–21.

[21] N. F. Kasri, M. A. M. Piah, and Z. Adzis, "Compact High-Voltage Pulse Generator for Pulsed Electric Field Applications: Lab-Scale Development," *Journal of Electrical and Computer Engineering*, vol. 2020, pp. 1–12, Sep. 2020, https://doi.org/10.1155/2020/6525483.

[22] D. Redondo, M. E. Venturini, E. Luengo, J. Raso, and E. Arias, "Pulsed electric fields as a green technology for the extraction of bioactive compounds from thinned peach by-products," *Innovative Food Science & Emerging Technologies*, vol. 45, pp. 335–343, Feb. 2018, https://doi.org/10.1016/j.ifset.2017.12.004.

[23] V. Novickij *et al.*, "High-frequency submicrosecond electroporator," *Biotechnology & Biotechnological Equipment*, vol. 30, no. 3, pp. 607–613, May 2016, https://doi.org/10.1080/13102818.2016.1150792.

[24] K. Lerchenmüller, M. Weimert, and T. Skowronek, "Ignition coils," in *Gasoline Engine Management*, K. Reif, Ed. Wiesbaden: Springer Fachmedien Wiesbaden, 2015, pp. 162–177.

[25] B. V. Malozyomov, A. V. Myatezh, and I. O. Korovin, "Diagnosis and reliability improvement of internal combustion engine ignition coil," *IOP Conference Series: Earth and Environmental Science*, vol. 194, Nov. 2018, Art. no. 052015, https://doi.org/10.1088/1755-1315/194/5/052015.

[26] A. I. Pressman, *Switching power supply design*, 3rd ed. New York: McGraw-Hill, 2009.

[27] K. Reif, Ed., *Gasoline Engine Management: Systems and Components*. Wiesbaden: Springer Fachmedien Wiesbaden, 2015.

[28] J. L. Blackburn and T. J. Domin, *Protective relaying: principles and applications*, Fourth edition. Boca Raton: CRC Press, Taylor & Francis Group, 2014.

[29] S. Takahashi, K. Wada, H. Ayano, S. Ogasawara, and T. Shimizu, "Review of Modeling and Suppression Techniques for Electromagnetic Interference in Power Conversion Systems," *IEEJ Journal of Industry Applications*, vol. 11, no. 1, pp. 7–19, Jan. 2022, https://doi.org/10.1541/ieejjia.21006800.

[30] A. V. Myatezh, L. I. Kochetkova, E. V. Akifeva, and A. V. Ivanov, "Promising algorithm for diagnosing vehicle ignition coils," *Journal of Physics: Conference Series*, vol. 1333, no. 6, Oct. 2019, Art. no. 062016, https://doi.org/10.1088/1742-6596/1333/6/062016.

[31] D. D. Tung and N. M. Khoa, "An Arduino-Based System for Monitoring and Protecting Overvoltage and Undervoltage," *Engineering, Technology & Applied Science Research*, vol. 9, no. 3, pp. 4255–4260, Jun. 2019, https://doi.org/10.48084/etasr.2832.

[32] R. C. Jaeger and T. N. Blalock, *Microelectronic circuit design*, 4th ed. New York: McGraw-Hill, 2011.

[33] J. Spidlen *et al.*, "Data File Standard for Flow Cytometry, Version FCS 3.2," *Cytometry Part A*, vol. 99, no. 1, pp. 100–102, Jan. 2021, https://doi.org/10.1002/cyto.a.24225.

[34] A. Darmawan, H. D. Kusumaningrum, N. Wulandari, S. Nurjanah, and A. T. Sugiarto, "Effect of pulsed electric field on the number and cell membrane of Vibrio parahaemolyticus in salted squid," *Jurnal Pengolahan Hasil Perikanan Indonesia*, vol. 28, no. 6, pp. 559–573, Jul. 2025, https://doi.org/10.17844/jphpi.v28i6.63292.

[35] L. Li, R. Yang, and W. Zhao, "The Effect of Pulsed Electric Fields (PEF) Combined with Temperature and Natural Preservatives on the Quality and Microbiological Shelf-Life of Cantaloupe Juice," *Foods*, vol. 10, no. 11, Oct. 2021, Art. no. 2606, https://doi.org/10.3390/foods10112606.